Computer Assisted Mechanics and Engineering Sciences, **13**: 3–19, 2006.

Application of thermographic fields in identification of structural properties and defects

Krzysztof Dems
Department of Technical Mechanics, Technical University of Łódź
Żeromskiego 116, Łódź, Poland

Zenon Mróz
Institute of Fundamental Technological Research, PAS
Świętokrzyska 21, Warsaw, Poland

(Received in the final form February 15, 2006)

The detection of defects as well as their location, orientation and size is performed using measurements of surface temperature either at some selected points or on selected surface areas or lines. The response temperature of a structure is caused by statically, quasi-statically or dynamically applied thermal load on some structural boundary parts or within its domain. On the basis of results of measurements, an inverse heat transfer problem is formulated for a model structure and next solved. The inverse solution is constructed by minimizing the properly defined distance norm of measured and model temperatures. The model temperature distribution is calculated using the finite element model of a structure, while in minimizing the distance norm functional the gradient-oriented methods are used. The proper sensitivities of introduced identification functional are also derived. Some simple examples illustrate the applicability of the proposed approach.

Keywords: identification, sensitivity, thermographic methods, path-independent integrals

1. Introduction

The prediction of structural properties, and in particular of location and size of voids, inclusions or any other kind of possible damage in existing engineering structures is of great importance from the point of view of their serviceability and safety. There exist many different approaches to analyze and identify the structural behaviour during service life of engineering structure. For instance, visual inspection and extensive testing can be employed to locate and measure the degradation of structure by non-destructive techniques such as acoustic emission, ultrasonic methods, modal testing or thermographic methods. There are numerous papers devoted to these classes of problems. An extensive review of damage identification techniques in structural and mechanical systems, based on dynamic response of a structure, was provided by Doebling *et al.* [6]. Nowadays, the most promising techniques of damage identification seem to be steady or transient thermographic methods based on temperature measurements. Using the thermographic methods, the temperature distribution within structural element, constituting the basic information for this approach, can be caused by both steady-state and transient thermal fields applied to inspected structure as well as by impulse or periodic thermal loading.

In the present paper, we shall study the detection of inclusion or voids by the analysis of steady-state or transient thermal response of structure, in particular the temperature distribution along its external boundaries caused by applied heat sources within structural domain or applied temperatures on some parts of its boundaries. In fact, temperature distribution varies with structural conductivity and its variation can be used in order to identify the variation of conductivity matrix

associated with void or defect location, orientation and size. The thermal loading in the form of pointwise or volumetric heat source as well as fixed temperature at some points or surface areas can be caused by thermal process within structure subjected to service load (*passive thermography*) or this loading can be forced exclusively for identification purposes (*active thermography*).

Two most typical identification problems that should be of interest are: (i) specification of a single void or defect with its size, location and orientation as unknown parameters and (ii) specification of distributed defects within a structure regarded as a distributed conductivity reduction when compared to homogenous structure or to the structure at its initial working conditions. Thus, one can observe either the forming of new defects or the progress in their growth during service life of structure as the result of non-destructive inspection based on thermal measurements.

The case of active thermography will be assumed in the present analysis and then the thermal load is applied exclusively for identification purposes. However, in the case of passive thermography, the identification procedure will be quite similar. The detection of surface, subsurface or internal inclusions, voids or cracks as well as their location, orientation and size can be performed using infrared measurements of surface temperature either at some selected points or on selected surface areas or lines. In order to increase the number of available measurement data, the thermal multi-loading case is considered. The several thermal loading cases are implemented either in the form of consecutively applied several increasing steady-state thermal loadings or in the form of transient loading and measurement of temperature within assumed time period $(t_0,\ t_f)$ or at consecutively selected time instances. On the basis of results of measurements, an inverse heat transfer problem is next formulated and solved. In order to determine the location, orientation and size of single or multiple defects, the properly defined distance norm between measured and model temperatures is formulated. Minimization of this norm will result in estimating location, orientation and size of void or defect.

Since the measurements are available mainly on the boundary surface of a structure, the identification functional will be constructed either on the whole surface or on its portion, as well as at some selected surface points or along specified surface lines. Performing the thermal analysis of a structure with void or inclusion, its finite element model is constructed and the predicted temperature distribution is next used in the identification procedure. The inverse solution can be constructed by minimizing the introduced distance norm of measured and model temperatures.

In simple examples verifying the applicability of presented approach, the infrared measurements will be numerically simulated. However, to make the simulation more realistic, some random error will be introduced into simulated measurements in order to model the unavoidable tolerance of real measurement.

2. Formulation of heat transfer problem

Since the identification procedure will be based on thermal measurements on structural surfaces, let us formulate the basic equations describing heat transfer problem within inspected structure. Consider therefore a two-dimensional structure, Fig. 1, occupying the domain Ω bounded by the external boundary $\Gamma = \Gamma_T \cup \Gamma_q \cup \Gamma_h$. Let us assume, that at any time instant t the temperature T is prescribed on the boundary portion Γ_T (Dirichlet condition), whereas the heat flux q_n proportional to normal gradient of temperature field (Neumann condition) is specified on the boundary portion Γ_q. On the remaining boundary portion Γ_h the heat convection with environmental temperature T_∞ (third type or Henkel condition) is assumed. Moreover, the initial temperature distribution at time $t = 0$ is also assumed to be known within structure domain. Thus, the temperature distribution within a model of inspected structure will be calculated considering the transient heat transfer problem described by the following set of heat balance and conduction equations,

$$\left.\begin{aligned} -\operatorname{div}\mathbf{q}(\mathbf{x},t,\mathbf{b}) + f(\mathbf{x}) &= c(\mathbf{x},\mathbf{b})\dot{T}(\mathbf{x},t,\mathbf{b}) \\ \mathbf{q}(\mathbf{x},t,\mathbf{b}) &= -\mathbf{A}(\mathbf{x},\mathbf{b})\cdot\nabla T(\mathbf{x},t,\mathbf{b}) \end{aligned}\right\} \quad \text{in } \Omega\times(0,t_f), \tag{1}$$

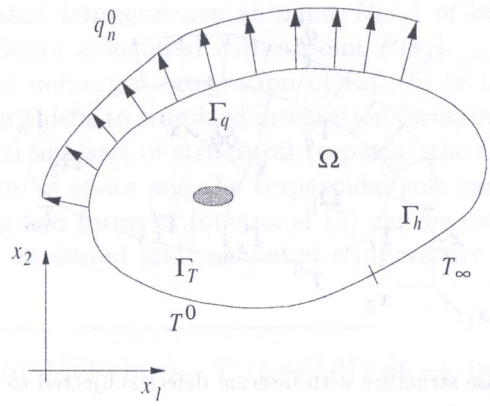

Fig. 1. Identified structure with internal defect subjected to thermal loading

supplemented with boundary and initial conditions in the form

$$\begin{aligned} &T(\mathbf{x},t,\mathbf{b}) = T^0(\mathbf{x},t) && \text{on } \Gamma_T \times (0,t_f),\\ &q_n(\mathbf{x},t,\mathbf{b}) = \mathbf{n}\cdot\mathbf{q} = q_n^0(\mathbf{x},t) && \text{on } \Gamma_q \times (0,t_f),\\ &q_n(\mathbf{x},t,\mathbf{b}) = \mathbf{n}\cdot\mathbf{q} = h[T(\mathbf{x},t,\mathbf{b}) - T_\infty(\mathbf{x},t)] && \text{on } \Gamma_h \times (0,t_f), \end{aligned} \tag{2}$$

and

$$T(\mathbf{x},0,\mathbf{b}) = T_0(\mathbf{x}) \quad \text{in } \{\Omega\times(0)\}\cup\{\Gamma\times(0)\}, \tag{3}$$

where $T(\mathbf{x},t,\mathbf{b})$ and $\mathbf{q}(\mathbf{x},t,\mathbf{b})$ denote the temperature field and heat flux vector within problem domain Ω bounded by the external boundary $\Gamma = \Gamma_T \cup \Gamma_q \cup \Gamma_h$, cf. Fig. 1, $\dot{T}$ denotes the temperature rate, $\mathbf{A}(\mathbf{x},\mathbf{b})$ and $c(\mathbf{x},\mathbf{b})$ are the material conductivity matrix and material heat capacity, respectively and $h(\mathbf{x},\mathbf{b})$ is a convection coefficient. Moreover, we assume that the boundary and initial conditions of the problem considered are given in advance and are design independent.

A structure with voids or cracks can be treated as occupying the multi connected domain Ω, for which the heat transfer phenomena are described by Eqs. (1)–(3). On the other hand, the inclusion or material defect within structural domain can be modeled by introducing two subdomains Ω_1 and Ω_2, so that $\Omega = \Omega_1 \cup \Omega_2$ and Ω_1 is a structure domain with conductivity matrix $\mathbf{A}_1$ while subdomain Ω_2 with conductivity matrix $\mathbf{A}_2$ represents the inclusion or defect within structure domain. In such case we should assume that two-phase domain of structure is considered and then the set of state equations (1) together with boundary and initial conditions (2) and (3) have to be supplemented with additional conditions, which are satisfied on the interface separating two subdomains Ω_1 and Ω_2, cf. Fig. 2, namely

$$\left.\begin{aligned} &\langle T^s(\mathbf{x},t,\mathbf{b})\rangle = 0\\ &\langle q_n^s(\mathbf{x},t,\mathbf{b})\rangle = \mathbf{n}\cdot\langle \mathbf{q}^s(\mathbf{x},t,\mathbf{b})\rangle = 0\\ &\text{and}\\ &\langle \nabla T^s(\mathbf{x},t,\mathbf{b})\rangle = \mathbf{n}\cdot\langle T^s_{,n}\rangle\\ &\langle \mathbf{q}^s(\mathbf{x},t,\mathbf{b})\rangle = -\langle \mathbf{A}\rangle\cdot\nabla_\Gamma T^s - \mathbf{n}\cdot\langle \mathbf{A}T^s_{,n}\rangle \end{aligned}\right\} \quad \text{on } \Gamma_s\times(0,t_f). \tag{4}$$

Here $\langle * \rangle$ denotes the jump of enclosed quantity on interface Γ_s, calculated as its difference on both sides of Γ_s, $\nabla_\Gamma T^s$ is a gradient of interface temperature T^s in plane tangent to interface and $T^s_{,n}$ denotes the normal gradient of the temperature field on Γ_s.

The identification of location, orientation and size of structural defect correspond to the case of shape modification of external or internal boundaries of structure and therefore the techniques applied in structural identification procedures are similar to those applied in problems of structural boundary modifications and associated optimization problems. The detailed analysis associated with

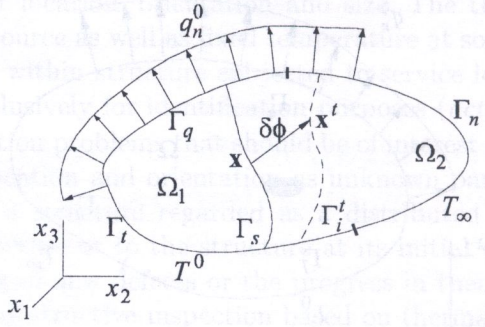

Fig. 2. Two-phase structure with internal defect subjected to thermal loading

shape modification and optimal design for problem described by Eqs. (1)–(3) was performed in [4], whereas the steady state problem for structures with interfaces was discussed in [2, 3]. In the present paper we will follow the analysis presented in [2–4] for the case of structural shape optimization with a particular form of the objective functional playing now the role of identification functional. Some specific forms of this functional will be discussed in the next Section.

3. Identification functional

In this paper the identification problem associated with shape and thermal properties of the inspected structure is considered. To identify the shape (within the assumed class of shapes) and location of defect, the identification functional in the form of proper distance norm between temperature fields within the model and real structure should be introduced. In particular, the size, position and orientation of defect can be identified using this procedure. In general, the identification functional can be assumed in the form of time and space integral, given in the form, cf. [5],

$$I(T, T^r, \mathbf{b}) = \int_{t_0}^{t_f} \int_{\Gamma(\mathbf{b})} \Phi[T(t, \mathbf{b}, s), T^r(t, s)] \, \mathrm{d}\Gamma_r \mathrm{d}t \rightarrow \min, \tag{5}$$

where Φ is an arbitrary function depending on the predicted and measured temperatures $T(t, \mathbf{b}, s)$ and $T^r(t, s)$ within assumed time period (t_0, t_f) and Γ_r denotes the boundary portion on which the non-vanishing space functional is defined with s denoting its boundary coordinate. The set $\mathbf{b}$ of time independent design parameters specifies the structural shape. In particular the design parameters can specify the position, orientation and scale change of optimized or identified structural boundary. Thus, we use the time window of bandwidth $t_f - t_0$ in order to gather the information required for the identification procedure. Both the initial and final times t_0 and t_f can be the same or different from the initial and final times of considered transient heat transfer problem. The extension of our analysis to the case of more general form of functional (5) involving also the functional defined within the structural domain Ω is straightforward and will be presented in consecutive papers.

Instead of time integral in Eq. (5), also the summation of space integral over some selected time instants t_k can be used in formulation of the behavioural functional, namely

$$I(T, T^r, \mathbf{b}) = \sum_{k=1}^{n} \xi_k \int_{\Gamma(\mathbf{b})} \Phi[T(t_k, \mathbf{b}, s), T^r(t_k, s)] \, \mathrm{d}\Gamma_r \rightarrow \min, \tag{6}$$

where the summation in Eq. (6) is applied on assumed number of time instances t_k $(k = 1, \ldots, n)$ and ξ_k denote some weighting factors. Also, instead of calculating the surface integral in Eq. (6), the temperature at some selected points $P(s_j)$, where s_j $(j = 1, \ldots, m)$ denotes the boundary coordinate, can be used in defining this functional. In this case, instead of Eq. (6), we can write

$$I(T, T^r, \mathbf{b}) = \sum_{k=1}^{n} \xi_k \sum_{j=1}^{m} \varsigma_j \Phi[T_{kj}(\mathbf{b}), T_{kj}^r] \rightarrow \min, \tag{7}$$

where T_{kj} denote the calculated temperatures at point $P(s_j)$ of boundary Γ_r in time instant t_k and ς_j denote the weighting factor associated with a point $P(s_j)$.

Let us note that in case of numerical integration of Eq. (5) in time or in time and space, the expressions (6) and (7) are equivalent to standard integration formulae. For instance, using the finite element approach in numerical analysis of structural response, the Gaussian integration procedure is typically used for integration in space and the trapezoidal rule can be used for time integration.

In particular, the following two forms of functional (5) can be considered. The first one is associated with distance norm of measured and calculated temperature fields and can be expressed in the form

$$I(T,T^r,\mathbf{b}) = \int_{t_0}^{t_f} \sqrt{\int_{\Gamma(\mathbf{b})} \alpha(s)\,[T(t,\mathbf{b},s) - T^r(t,s)]^2\,\mathrm{d}\Gamma_r}\,\mathrm{d}t \;\to\; \min, \tag{8}$$

where $\alpha(s)$ is a weighting function, which can magnify or weaken the difference between the model and measured temperature on some portion of structural boundary. The other form of identification functional can be based on measurement of temperature differences for structure or its model at initial and actual conditions, induced by the change of thermal properties of structure during its service life due to possible damage. Denoting these differences by ΔT^r and ΔT, respectively, the following identification functional can be introduced,

$$I(T,T^r,\mathbf{b}) = -\int_0^{t_f} \frac{\int_{\Gamma(\mathbf{b})} \Delta T(t,\mathbf{b},s)\Delta T^r(t,s)\,\mathrm{d}\Gamma_r}{\sqrt{\int_{\Gamma(\mathbf{b})} \{\Delta T(t,\mathbf{b},s)\}^2\,\mathrm{d}\Gamma_r \int_{\Gamma(\mathbf{b})} \{\Delta T^r(t,\mathbf{b},s)\}^2\,\mathrm{d}\Gamma_r}}\,\mathrm{d}t \;\to\; \min. \tag{9}$$

The space integral in Eq. (9) indicates the correlation between measured and model temperature differences for actual and initial (perfect) structures. The value of this integral lies between -1 and $+1$, where -1 indicates the exact match, 0 corresponds to no correlation between model and measured temperature changes and $+1$ indicates the antisymmetric correlation between model and real structure at given time instant t.

The equivalent discrete form of functional (8) and (9), corresponding to general expressions (6) and (7), can be written as

$$\begin{aligned} I(T,T^r,\mathbf{b}) &= \sum_{k=1}^{n} \xi_k \sqrt{\int_{\Gamma(\mathbf{b})} \alpha(s)\,[T(t_k,\mathbf{b},s) - T^r(t_k,s)]^2\,\mathrm{d}\Gamma_r} \\ &= \sum_{k=1}^{n} \xi_k \sqrt{\sum_{j=1}^{m} \varsigma_{uj}\alpha(s)\,[T_{kj}(\mathbf{b}) - T^r_{kj}]^2} \;\to\; \min, \end{aligned} \tag{10}$$

and

$$\begin{aligned} I(T,T^r,\mathbf{b}) &= -\sum_{k=1}^{n} \frac{\int_{\Gamma(\mathbf{b})} \Delta T(t_k,\mathbf{b},s)\,\Delta T^r(t_k,s)\,\mathrm{d}\Gamma_r}{\sqrt{\int_{\Gamma(\mathbf{b})} \{\Delta T(t_k,\mathbf{b},s)\}^2\,\mathrm{d}\Gamma_r \int_{\Gamma(\mathbf{b})} \{\Delta T^r(t_k,\mathbf{b},s)\}^2\,\mathrm{d}\Gamma_r}} \\ &= -\sum_{k=1}^{n} \frac{\sum_{j=1}^{m} \varsigma_j\,\Delta T_{kj}(\mathbf{b})\,\Delta T^r_{kj}}{\sqrt{\sum_{j=1}^{m} \varsigma_j \{\Delta T_{kj}(\mathbf{b})\}^2 \sum_{j=1}^{m} \varsigma_j \{\Delta T^r_{kj}\}^2}} \;\to\; \min. \end{aligned} \tag{11}$$

To identify the defect position, size and other parameters, the identification functional (5) has to be minimized. Using any gradient oriented minimization techniques, there is a need of calculating the desired sensitivities of functional (5) with respect to a set $\mathbf{b}$ of parameters defining location, orientation and other parameters of defect within structure domain. In performing this calculation, a direct or adjoint approach to sensitivity analysis for transient heat transfer problem can be applied. The detailed analysis for this case was discussed by Dems and Rousselet in [4] and we can recall

here the obtained results. In particular case of void translation or rotation within structure domain, a new class of path-independent sensitivity integrals will be also derived. This class of sensitivity integrals will allow for integration of desired sensitivity expressions along paths situated far from areas of rapid changes of temperature gradient caused by voids or cracks within structure domain. In particular, these sensitivity integrals can be calculated along external boundary of a structure, where the measured temperature distribution is easily available.

4. Sensitivity of identification functional

Let us assume that the functional (5) is defined within varying domain Ω of, in general, a multi-phase structure with internal surfaces Γ_s bounded by external boundary Γ. The thermal properties of structure are assumed to be design independent, and only the shape, size, location and orientation of external and internal structural boundaries can undergo modifications. The infinitesimal variation of structural domain is described by a set $\mathbf{b}$ of design parameters as follows,

$$\Omega \to \Omega' : \mathbf{x}^t = \mathbf{x} + \mathbf{v}^p(\mathbf{x}, \mathbf{b})\, \delta b_p\,, \tag{12}$$

where $\mathbf{v}^p(\mathbf{x}, \mathbf{b})$ denotes a transformation velocity field associated with shape parameter b_p and satisfying proper boundary conditions. In the case of external boundary modification, the normal component of transformation velocity field should vanish only on fixed part of external boundary, allowing for shape modification of remainder boundary portion. On the other hand, in the case of interface modification, the normal component of transformation velocity field should vanish on the entire external boundary, allowing only for modification of interior of structural domain and as the result for modification of shape of structural interfaces.

The first-order sensitivities of functional (5) with respect to components b_p of design vector $\mathbf{b}$ describing the variation of structural domain can be written as

$$I_p = \int_0^{t_f} G_p \, \mathrm{d}t, \qquad p = 1, 2, \ldots, P, \tag{13}$$

where the sensitivity G_p is expressed in the form, cf. [3],

$$G_p = \left[\int_{\Gamma(\mathbf{b})} \Phi[T(t, \mathbf{b}, s), T^r(t, s)] \, \mathrm{d}\Gamma_r \right]_p = \int_{\Gamma(\mathbf{b})} [\Phi_{,T} T_p + \Phi(\mathrm{div}_\Gamma \mathbf{v}^p - 2H\mathbf{v}^p \cdot \mathbf{n})] \, \mathrm{d}\Gamma_r\,, \tag{14}$$

and T_p denotes the sensitivity (total material derivative) of temperature field, whereas $\mathrm{div}_\Gamma(*)$ denotes the divergence of enclosed quantity in plane tangent to Γ and $2H$ denotes the mean curvature of Γ_r.

The total material derivative of temperature field T with respect to any components b_p of a set $\mathbf{b}$ equals

$$T_p = T_{,p} + \nabla T \cdot \mathbf{v}^p \tag{15}$$

where the local derivative $T_{,p} = \partial T / \partial b_p$ is calculated for a fixed space position $\mathbf{x}$. Using (15) in Eq. (14) the equivalent expression for sensitivity G_p can be obtained, namely

$$G_p = \int_{\Gamma(\mathbf{b})} [\Phi_{,T}(T_{,p} + \nabla T \cdot \mathbf{v}^p) + \Phi(\mathrm{div}_\Gamma \mathbf{v}^p - 2H\mathbf{v}^p \cdot \mathbf{n})] \, \mathrm{d}\Gamma_r\,. \tag{16}$$

The sensitivity $I_{,p}$ defined by Eq. (13), with G_p expressed by Eq. (14) or (16) can be, in general, calculated using the direct or adjoint approaches.

The direct method of sensitivity analysis results in direct calculating the total or local sensitivities of temperature field and then using these sensitivities in expressions (14) or (16) in order to calculate G_p and next, by means of Eq. (13), to calculate the desired sensitivities I_p of identification functional (5). To derive directly the sensitivities of temperature field T, the state equations

defining the primary heat transfer problem within structure domain should be differentiated with respect to the components of design vector $\mathbf{b}$, constituting the state equations for the set of additional heat transfer problems, each associated with particular component b_p of design vector $\mathbf{b}$ and independent of a particular form of the identification functional (5). For the case of modification of external structural boundary, differentiation of state equation (1) together with boundary and initial conditions (2) and (3) with respect to design parameter b_p, yields the following set of equations describing the additional transient heat transfer problem. The conduction equation, following from differentiation of Eq. (1), has the form

$$\left.\begin{aligned} -\operatorname{div}\mathbf{q}_{,p} &= c\dot{T}_{,p} \\ \mathbf{q}_{,p} &= -\mathbf{A}\cdot\nabla T_{,p} \end{aligned}\right\} \quad \text{in } \Omega\times(0,t_f), \tag{17}$$

whereas the boundary and initial conditions, following from differentiation of Eqs. (2) and (3), will be expressed as

$$\begin{aligned} &T_{,p} = -\nabla T\cdot\mathbf{v}^p && \text{on } \Gamma_T\times(0,t_f),\\ &q_{n,p} = \mathbf{n}\cdot\mathbf{q}_{,p} = -\nabla q_n\cdot\mathbf{v}^p + \mathbf{q}\cdot\nabla_\Gamma v_n^p && \text{on } \Gamma_q\times(0,t_f),\\ &q_{n,p} = \mathbf{n}\cdot\mathbf{q}_{,p} = h(T_{,p}-T_\infty^p),\quad T_\infty^p = -\tfrac{1}{h}\mathbf{q}_\Gamma\cdot\nabla_\Gamma v_n^p && \text{on } \Gamma_h\times(0,t_f), \end{aligned} \tag{18}$$

and

$$T_{,p} = -\nabla T_0\cdot\mathbf{v}^p \qquad \text{in } \{\Omega\times(0)\}\cup\{\Gamma\times(0)\}. \tag{19}$$

In the case of a two-phase structural domain considered, the primary heat transfer equations are supplemented by the interface conditions (4), and the equations of additional heat transfer problems have to be supplemented with conditions following from differentiation of Eq. (4), namely

$$\left.\begin{aligned} \langle T_{,p}^s\rangle &= -\langle T_{,n}^s\rangle v_n^p \\ \langle q_{n,p}^s\rangle &= -\langle q_{n,n}^s\rangle v_n^p + \langle\mathbf{q}_\Gamma^s\rangle\cdot\nabla_\Gamma v_n^p \end{aligned}\right\} \quad \text{on } \Gamma_s\times(0,t_f). \tag{20}$$

The solution of problems described by Eqs. (17)–(19) or (17)–(20) yields the sensitivity fields $T_{,p}$ and the desired sensitivities of identification functional can be calculated. The detailed analysis of direct approach to sensitivity analysis is presented, for instance, in [2–5]. However, one should note that the main disadvantage of such approach is a need of solution of a number of additional transient heat transfer problems that equals to number of design parameters used to identification of structural defect.

Much more challenging approach for deriving the sensitivities of identification functional is offered by the adjoint method of sensitivity analysis. Here, apart from solution of primary problem, one adjoint heat transfer problem should be formulated and solved in order to calculate the sensitivities (13). This adjoint problem, associated with particular form of identification functional (5), is defined by the following conduction equation, cf. [4],

$$\left.\begin{aligned} -\operatorname{div}\mathbf{q}^a(\mathbf{x},\tau,\mathbf{b}) &= cT^{a\prime}(\mathbf{x},\tau,\mathbf{b}) \\ \mathbf{q}^a(\mathbf{x},\tau,\mathbf{b}) &= -\mathbf{A}\cdot\nabla T^a(\mathbf{x},\tau,\mathbf{b}) \end{aligned}\right\} \quad \text{in } \Omega\times(0,t_f), \tag{21}$$

supplemented with boundary and initial conditions in the form:

$$\begin{aligned} &T^a(\mathbf{x},\tau,\mathbf{b}) = T^{a0}(\mathbf{x},\tau,\mathbf{b}) = 0 && \text{on } \Gamma_T\times(0,t_f),\\ &q_n^a(\mathbf{x},\tau,\mathbf{b}) = \mathbf{n}\cdot\mathbf{q}^a = q_n^{a0}(\mathbf{x},\tau,\mathbf{b}) = -\Phi_{,T}(\mathbf{x},t,\mathbf{b}) && \text{on } \Gamma_q\times(0,t_f),\\ &q_n^a(\mathbf{x},\tau,\mathbf{b}) = \mathbf{n}\cdot\mathbf{q}^a = h[T^a(\mathbf{x},\tau,\mathbf{b}) - T_\infty^a(\mathbf{x},\tau,\mathbf{b})] && \\ &T_\infty^a(\mathbf{x},\tau,\mathbf{b}) = \tfrac{1}{h}\Phi_{,T}(\mathbf{x},t,\mathbf{b}) && \text{on } \Gamma_h\times(0,t_f), \end{aligned} \tag{22}$$

and

$$T^a(\mathbf{x},0,\mathbf{b}) = T_0^a(\mathbf{x},\mathbf{b}) = 0 \qquad \text{in } \{\Omega\times(0)\}\cup\{\Gamma\times(0)\}, \tag{23}$$

where the time coordinate τ of adjoint problem is related to time t of primary problem through the relation

$$\tau = t_f - t \tag{24}$$

and $(*)' = \partial(*)/\partial\tau = -\partial(*)/\partial t$ denotes the differentiation with respect to adjoint time τ.

For the case of two-phase structural domain, when the primary heat transfer equations are supplemented with interface conditions (4), the equations of adjoint heat transfer problems have to be supplemented with conditions of the form

$$\left.\begin{aligned} &\langle T^{as}(\mathbf{x},\tau,\mathbf{b})\rangle = 0 \\ &\langle \nabla T^{as}(\mathbf{x},\tau,\mathbf{b})\rangle = \mathbf{n}\cdot\langle T^{as}_{,n}(\mathbf{x},\tau,\mathbf{b})\rangle \\ &\langle q^{as}_n(\mathbf{x},\tau,\mathbf{b})\rangle = \mathbf{n}\cdot\langle \mathbf{q}^{as}(\mathbf{x},\tau,\mathbf{b})\rangle = 0 \\ &\langle \mathbf{q}^{as}(\mathbf{x},\tau,\mathbf{b})\rangle = -\langle \mathbf{A}\cdot\nabla T^{as}(\mathbf{x},\tau,\mathbf{b})\rangle \end{aligned}\right\} \quad \text{on } \Gamma_s\times(0,t_f). \tag{25}$$

Using now the solutions of adjoint heat transfer problem (21)–(23) or (21)–(23), (25) and making use of the relation, cf. [4],

$$-\int_{\Omega(\mathbf{b})} T_{,p} c T^a \,\mathrm{d}\Omega\Big|_{t_0}^{t_f} + \int_0^{t_f}\left\{\int_{\Gamma_q(\mathbf{b})} T_{,p} q_n^{a0}\,\mathrm{d}\Gamma_q - \int_{\Gamma_h(\mathbf{b})} T^a_\infty h T_{,p}\,\mathrm{d}\Gamma_h - \int_{\Gamma_T(\mathbf{b})} q^a_n \nabla T\cdot\mathbf{v}^p\,\mathrm{d}\Gamma_T\right.$$
$$\left. - \int_{\Gamma_q(\mathbf{b})} T^a\left(\mathbf{q}_\Gamma\cdot\nabla_\Gamma v^p_n - \nabla_\Gamma q_n\cdot\mathbf{v}^p_\Gamma - q_{n,n}v^p_n\right)\mathrm{d}\Gamma_q + \int_{\Gamma_h(\mathbf{b})} T^a h T^p_\infty\,\mathrm{d}\Gamma_h\right\}\mathrm{d}t = 0, \tag{26}$$

the term containing the derivative $T_{,p}$ in Eq. (16) can be eliminated and expressed in terms of primary and adjoint solutions. Thus, following the analysis presented in [4], the sensitivities (13) for the case of external boundary modification can be finally expressed in the form

$$I_p = -\int_{\Omega(\mathbf{b})} cT^a\nabla T\cdot\mathbf{v}^p\,\mathrm{d}\Omega\Big|_{t=t_0}$$
$$+\int_0^{t_f}\left\{-\int_{\Gamma_T}\left(\Phi_{,T}+q^a_n\right)\left(\nabla_\Gamma T\cdot\mathbf{v}^p_\Gamma + T_{,n}v^p_n\right)\mathrm{d}\Gamma_T - \int_{\Gamma_q(\mathbf{b})} T^a\left(\mathbf{q}_\Gamma\cdot\nabla_\Gamma v^p_n - \nabla q_n\cdot\mathbf{v}^p\right)\mathrm{d}\Gamma_q\right.$$
$$\left.+\int_{\Gamma_h(\mathbf{b})} T^a h T^p_\infty\,\mathrm{d}\Gamma_h + \int_{\Gamma(b)}\left(\Phi_{,n} - 2H\Phi\right)v^p_n\,\mathrm{d}\Gamma + \int_{\Sigma(\mathbf{b})}\langle\Phi\mathbf{v}^p_\Gamma\cdot\mathbf{s}\rangle\mathrm{d}\Sigma\right\}\mathrm{d}t, \tag{27}$$

where the function Φ and primary fields T, $\mathbf{q}$ and f are calculated at time t and adjoint fields T^a and q^a_n are calculated in the corresponding time $\tau = t_f - t$. The last integral on the right-hand side of Eq. (27) is expanded over all intersection curves of partially smooth surface Γ and unit vector $\mathbf{s}$ normal to Σ and tangential to Γ is defined by

$$\mathbf{s}^- = \mathbf{a}\times\mathbf{n}^-, \qquad \mathbf{s}^+ = \mathbf{a}\times\mathbf{n}^+, \tag{28}$$

where $\mathbf{a}$ denotes the unit tangent vector on Σ, while $(*)^-$ and $(*)^+$ denote the enclosed quantity calculated along Σ on the left and right sides of Γ.

On the other hand, when the interface Γ_s undergoes the modification with external boundary fixed, instead of Eq. (27), we obtain

$$I_p = -\int_{\Omega(\mathbf{b})} cT^a\nabla T\cdot\mathbf{v}^p\,\mathrm{d}\Omega\Big|_{t=0}$$
$$+\int_0^{t_f}\left\{\int_{\Gamma_s(b)}\left(-\langle T^s_{,n}\rangle q^{as}_n + \langle q^s_{n,n}\rangle T^{as}v^p_n - T^{as}\langle\mathbf{q}^s_\Gamma\rangle\cdot\nabla_\Gamma v^p_n\right)\mathrm{d}\Gamma_s\right\}\mathrm{d}t. \tag{29}$$

The above derived sensitivity expressions, apart from using sensitivity analysis approaches, enable to conduct any gradient oriented identification procedure baseed on a particular form of identification functional (5) and arbitrary modification of shape, size, location and orientation of void, inclusion or defect located within structure domain.

Let us note at this point of analysis, that the transition of identification procedure based on transient heat transfer problem to the case of steady-state or quasi steady-state case will require neglecting time integrals and time derivatives in formulated state equations and derived sensitivity expressions.

5. Functional variation associated with translation and rotation of structural defect

Consider now two most fundamental modifications of structure domain associated with presence of void or defect, namely its translation and rotation. Let us derive the particular form of sensitivity expressions of an arbitrary surface functional (5) associated with these modifications. Once again, the first variation of (5) takes the form (13), where the sensitivities with respect to design parameters for an arbitrary domain variation are obtained using the adjoint approach and are expressed, for instance, by Eq. (27). Now we will particularize this expression for the class of above mentioned domain variation. First of all, let us assume the homogeneous initial conditions for primary problem, i.e. $T(\mathbf{x}, 0, \mathbf{b}) = 0$ in $\{\Omega \times (0)\} \cup \{\Gamma \times (0)\}$, and write the expression (27) in the global Cartesian coordinate system within given space-time, namely

$$I_p = \int_{t_0}^{t_f} \left\{ \int_{\Gamma(\mathbf{b})} \left\{ \left[(fT^a - c\dot{T}T^a + q_i T^a_{,i}) n_k - (q_l T^a_{,k} + q^a_l T_{,k}) n_l \right] v^p_k \right. \right.$$
$$\left. \left. + (n_i q_i T^a - \Phi)(n_k n_l - \delta_{kl})\, v^p_{k,l} \right\} \mathrm{d}\Gamma \right\} \mathrm{d}t \tag{30}$$

Consider now the translation of structure domain, Fig. 3. In this case the design parameters b_p are reduced to the two components of a constant translation vector $\mathbf{a}$ and then the transformation velocity fields associated with components a_p are reduced to constant fields $v^p_k = \delta_{pk}$ over domain Ω and its boundary Γ. Since the boundary conditions of primary problem (1) are also translated correspondingly, then their variations vanish and sensitivity of functional (5) following from Eq. (30) can be expressed in the form

$$(I^T_p)_\Gamma = \int_{t_0}^{t_f} (G^T_p)_\Gamma \, \mathrm{d}t$$
$$= \int_{t_0}^{t_f} \left\{ \int_{\Gamma(\mathbf{b})} \left\{ \left[(fT^a - c\dot{T}T^a + q_l T^a_{,l})\, \delta_{ip} - (q_l T^a_{,p} + q^a_l T_{,p})\, \delta_{il} \right] n_i \right\} \mathrm{d}\Gamma \right\} \mathrm{d}t. \tag{31}$$

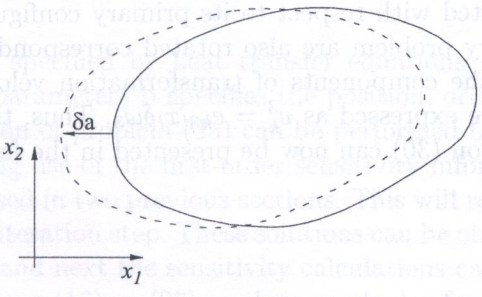

Fig. 3. Translation of structural domain

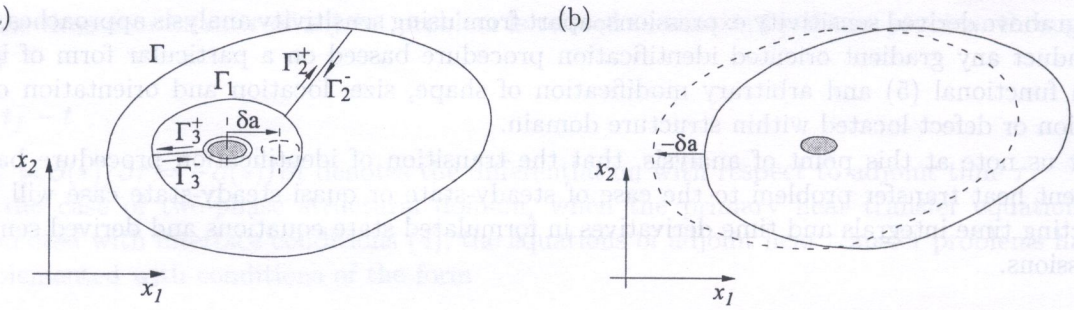

Fig. 4. Translation of inhomogeneity within a structure with fixed external boundary (a) and opposite translation of external boundary with fixed inhomogeneity (b)

Following the analysis presented in [1], it is easy to show *for a homogeneous domain* Ω *and constant source term* f, that *the integral* (31) *vanishes for any closed surface within the problem domain, yielding* $(G_p^T)_\Gamma = 0$ *and* $(I_p^T)_\Gamma = 0$, $p = 1, 2, 3$.

For a non-homogeneous domain, the integral (31) represents the sensitivity of the functional I due to infinitesimal translation of the boundary with respect to inhomogeneity. Alternatively, we can consider the translation of inhomogeneity or internal void with external boundary fixed, cf. Fig. 4. In Fig. 4a, the external boundary does not vary and the void of surface Γ_0 translates through the distance $\delta\mathbf{a}$ within the homogeneous domain. The variation of I can now be calculated by considering the integral (31) along the void surface Γ_0. For the surface Γ_0, on which $q_n = q_n^a = 0$, the expression (31) is simplified, namely

$$(I_p^T)_{\Gamma_0} = \int_{t_0}^{t_f} (G_p^T)_{\Gamma_0}\, \mathrm{d}t, \qquad (G_p^T)_{\Gamma_0} = \int_{\Gamma(\mathbf{b})} (fT^a - c\dot{T}T^a + q_l T_{,l}^a)\, n_p\, \mathrm{d}\Gamma. \tag{32}$$

Consider now an arbitrary closed surface Γ_1 enclosing the cavity and connect it to the cavity surface Γ_0 by the cuts Γ_3^- and Γ_3^+. Since the integral G_p^T taken along the surface $\Gamma_1 \cup \Gamma_3^- \cup \Gamma_0 \cup \Gamma_3^+$ vanishes and the integrals along Γ_3^- and Γ_3^+ cancel, we obtain

$$\begin{aligned} &(G_p^T)_{\Gamma_0} + (G_p^T)_{\Gamma_1} = 0 \\ &(G_p^T)_{\Gamma_0} = -(G_p^T)_{\Gamma_1} = -\int_{\Gamma_1} \left[(fT^a - c\dot{T}T^a + q_l T_{,l}^a)\, \delta_{ip} - (q_l T_{,p}^a + q_l^a T_{,p})\, \delta_{il}\right] n_i\, \mathrm{d}\Gamma. \end{aligned} \tag{33}$$

The transition from Γ_1 to Γ can be performed similarly by cuts Γ_2^- + and Γ_2^+. An alternate way to calculate the variation of G and I is to consider the translation of the domain through the vector $-\delta\mathbf{a}$ with the cavity fixed in space, cf. Fig. 4b. The transition from the boundary surface Γ to an arbitrary closed surface Γ_1 enclosing the cavity or to the cavity surface Γ_0 is also obtained by considering the cuts between these surfaces. Thus, it is shown that the functional (31) associated with an arbitrary functional I can be taken along any arbitrary closed and piecewise smooth surface within the problem domain providing always the same value. In this sense, the functionals G_p^T and I_p^T are *path-independent.*

The similar property can be shown for the case of rotation of structure domain, cf. Fig. 5. Assume then that the domain $\Omega$is rotated with respect to its primary configuration along x_3 axis and the boundary conditions of primary problem are also rotated correspondingly. Denoting the infinitesimal rotation vector by $\delta\omega_3$, the components of transformation velocity field $\mathbf{v}^3$ associated with infinitesimal rotation vector are expressed as $v_k^3 = e_{k3l} x_l \delta\omega_3$. Thus, the sensitivity of functional I, following from general expression (30) can now be presented in the form

$$\begin{aligned} (I_3^R)_\Gamma &= \int_{t_0}^{t_f} (G_3^R)_\Gamma\, \mathrm{d}t \\ &= \int_{t_0}^{t_f} \left\{ e_{k3l} \int_{\Gamma(\mathbf{b})} \left\{ \left[(fT^a - c\dot{T}T^a + q_j T_{,j}^a)\, x_l \delta_{ki} - (q_j T_{,k}^a + q_j^a T_{,k})\, x_l \delta_{ji}\right] n_i \right\} \mathrm{d}\Gamma \right\} \mathrm{d}t. \end{aligned} \tag{34}$$

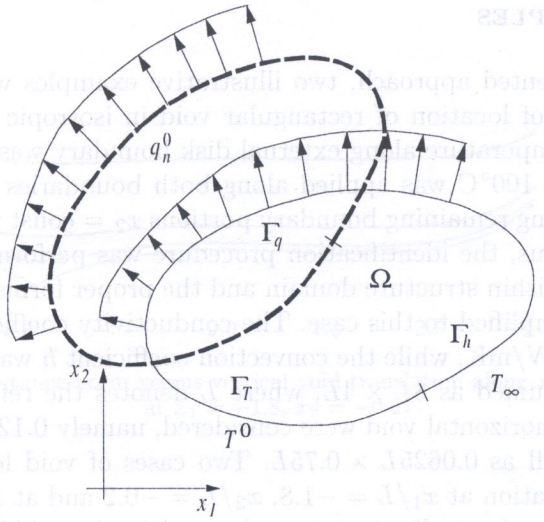

Fig. 5. Rotation of structural domain

Assuming now that the source term f of primary problem is constant within the *homogeneous* and *isotropic* domain Ω, it can be easily proved *that the surface integrals* $(G_3^R)_\Gamma$ *and* $(I_3^R)_\Gamma$ *defined by Eq.* (34) *vanish for any closed surface within the structure domain.* For the case of non-homogeneous domain, Eq. (34) represents the sensitivity of the functional I due to infinitesimal rotation of the boundary with respect to inhomogeneity. The transition of the integrals in Eq. (34) from external surface boundary Γ to an arbitrary closed surface within the non homogeneous domain Ω can be performed similarly as for the case of translation and then the integrals $(G_3^R)_\Gamma$ and $(I_3^R)_\Gamma$ can be considered as *path-independent.*

Two additional remarks should be stated at this point of analysis. Firstly, the combined transformation of problem domain consisting of simultaneous translation and rotation can be considered as a pure rotation with respect to properly selected center of rotation. The proof of these properties for a general case of behavioral functional I will follow the steps similar to those presented in [1]. Secondly, the transition of identification procedure based on transient heat transfer problem to the case of steady-state or quasi steady-state case will require, as stated in the previous section, neglecting time derivatives and omitting time integrals in presented formulation.

6. Identification procedure

The identification problem is thus formulated as follows,

$$\text{minimize } I(T, T^r, \mathbf{b}), \tag{35}$$

where temperature field T is specified by heat transfer equations (1)–(3) while T^r results from measurements and the set of parameters $\mathbf{b}$ specifies the position, orientation and other parameters of identified defect. The solution of problem (35) can be performed by means of any unconstrained minimization procedure making use of the first-order sensitivity information, which can be derived following the procedure proposed in two previous sections. This will require the solutions of primary and adjoint structures at each iteration step. These solutions can be obtained using the finite element model of identified structures and next the sensitivity calculations can be performed by calculating the either the general expressions (16) or (27) or their particular forms (31) or (34) along external boundary of a structure, where the measured temperatures are available for a real structure.

7. Illustrative examples

In order to justify the presented approach, two illustrative examples were considered. In the first example, the identification of location of rectangular void in isotropic disk shown in Fig. 6 using measurements of surface temperature along external disk boundary was performed. The prescribed constant temperature $T^0 = 100°\mathrm{C}$ was applied along both boundaries $x_1 = \text{const}$ and convection conditions were assumed along remaining boundary portions $x_2 = \text{const}$ with uniform environmental temperature $T_\infty = 0°\mathrm{C}$. Thus, the identification procedure was performed considering the steady-state case of heat transfer within structure domain and the proper forms of identification functional and its sensitivities were simplified to this case. The conductivity coefficient λ of disk material was assumed to be equal to 1.0 W/mK, while the convection coefficient h was equal to 5.0 $\mathrm{W/m^2K}$. The dimensions of disk were assumed as $8L \times 4L$, where L denotes the reference dimension, and four different sizes of vertical or horizontal void were considered, namely $0.125L \times 1.25L$, $0.125L \times 0.75L$ and $0.0625L \times 1.25L$ as well as $0.0625L \times 0.75L$. Two cases of void location within a 'real disk' were considered, namely location at $x_1/L = -1.8$, $x_2/L = -0.2$ and at $x_1/L = -1.8$, $x_2/L = -1.2$, respectively, with the origin of coordinate system located in the middle point of disk, cf. Fig. 6. The finite element model of disk consisted from 512 rectangular elements with total 2145 degrees of freedom (nodal temperatures).

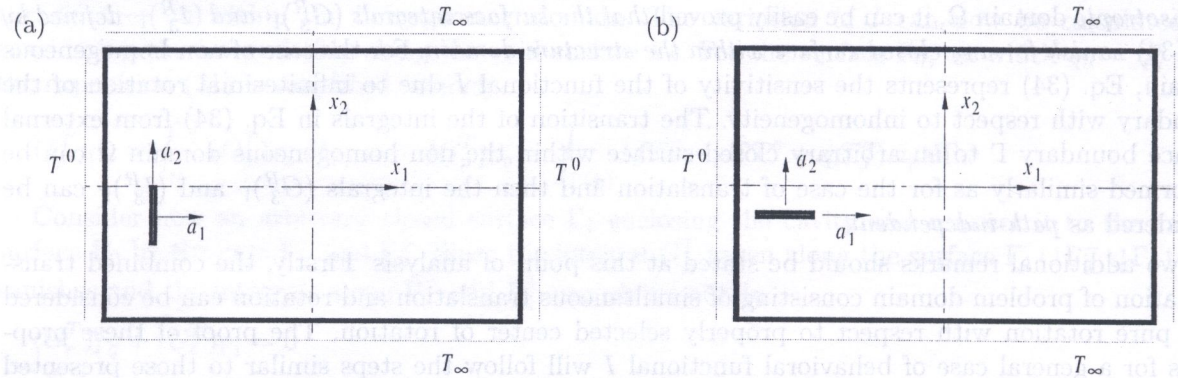

Fig. 6. Rectangular disk with translated (a) vertical void and (b) horizontal void

The measured temperature along boundaries $x_2 = \text{const}$ for 'real' disk was numerically simulated and some random absolute error of measured temperature distribution was introduced into simulation. To verify the usefulness of different identification functionals, the expression (8) or (9), simplified to steady-state case, was selected as the identification functional and then the location of void along x_1 and x_2 directions was identified. In each step of identification procedure the analysis of primary and adjoint problems was performed using the introduced finite element model of disk and sensitivity of respective functional were calculated using expression (31) simplified for the case of steady-state heat transfer problem.

Figures 7 and 8 show the plot of functional (8) versus the actual location of internal vertical void $0.0625L \times 1.25L$ within model disk for identification procedure based on temperature measurements with different level of random relative measurement error. Figure 7 corresponds to the case when the void in 'real' disk was located at $x_1/L = -1.8$, $x_2/L = -0.2$, whereas the case of real void location at $x_1/L = -1.8$, $x_2/L = -1.2$ is depicted in Figure 8. We can observe that there exists a minimum of functional (8) corresponding to void location in a model of disk, which is closed to void location in real structure. However, together with increasing error in measurement this minimum becomes more flat and then the identification of void location can be less accurate. Moreover, the quality of identification results depends also on relative location of real void with respect to the boundaries on which the measurement is performed. This phenomenon can be easily observed when Figures 7 and 8 are compared. It should be added, that the quality of identification depends also on the

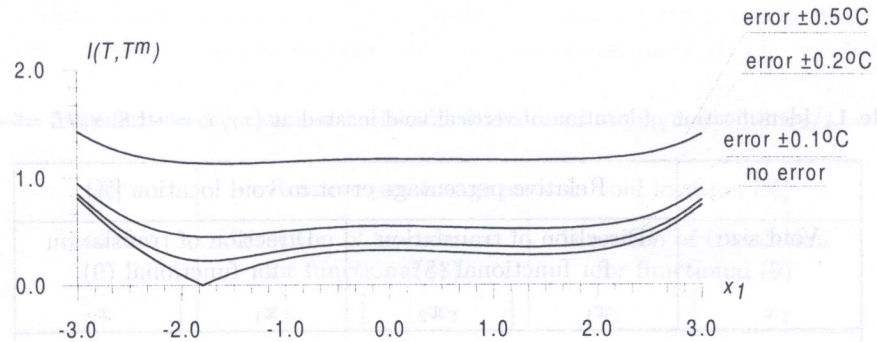

Fig. 7. Values of distance norm versus vertical void translation along x_1 axis (reference void at $x_1 = -1.8$, $x_2 = -0.2$)

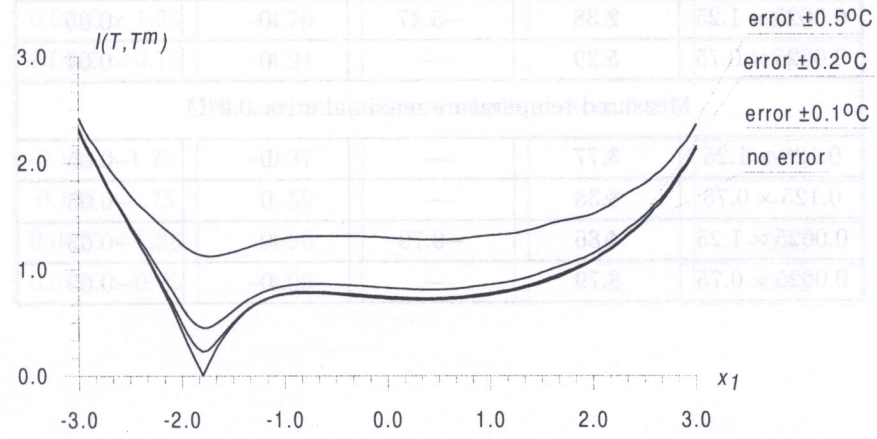

Fig. 8. Values of distance norm versus vertical void translation along x_1 axis (reference void at $x_1 = -1.8$, $x_2 = -1.2$)

form and number of thermal boundary conditions applied to the inspected structure. In the present example only one set of boundary conditions was used.

The identification procedure was performed using both above mentioned forms of identification functional with the absolute pseudo-random error of magnitude $\pm 0.1°C$ and $\pm 0.2°C$ introduced into measurement of temperatures. The results of one-parameter independent identification of void location along x_1 and x_2 axis for vertical void located in 'real' structure at $x_1/L = -1.8$, $x_2/L = -0.2$ and $x_1/L = -1.8$, $x_2/L = -1.2$ are shown in Tables 1 and 2, respectively. The similar results for horizontal void are presented in Tables 3 and 4. In all cases the quality of identification was evaluated on the basis of percentage error in void location, $100\% \times (x_{\text{iden}} - x_{\text{real}})/x_{\text{real}}$. The error not increasing 10% was assumed as the upper level of acceptable identification, and only results satisfying this constraint are presented in Tables 1, 2, 3 and 4.

The result of identification, based on measured temperature affected by error, can be treated as satisfactory in most cases. Particularly, for void location at $x_1/L = -1.8$, $x_2/L = -1.2$, which is relatively closed to boundary part on which the measurement was performed, we obtain the acceptable results even for high level of measurement error. However, for the case of void location at $x_1/L = -1.8$, $x_2/L = 0.2$, relatively farther located from structure boundary, the results of identification are burdened with greater error, and for greater error in measured temperature are simply unacceptable. This is mostly due to the fact, that the changes in temperature distribution along lower and upper boundary portions of a disk, caused by different location of void appearing deep inside the structure domain, are relatively small. By increasing the number of applied sets of different thermal boundary conditions we can probably help in better identification of void location in such cases.

Table 1. Identification of location of vertical void located at ($x_1/L = -1.8$, $x_2/L = -0.2$)

Void size	Relative percentage error in void location [%]			
	Direction of translation for functional (8)		Direction of translation for functional (9)	
	x_1	x_2	x_1	x_2
Measured temperature maximal error 0.1°C				
0.125 × 1.25	1.84	−8.25	0	−0.05
0.125 × 0.75	4.27	–	0	−0.03
0.0625 × 1.25	2.38	−5.47	0	0.05
0.0625 × 0.75	5.29	–	0	−0.04
Measured temperature maximal error 0.2°C				
0.125 × 1.25	3.77	–	0	−0.05
0.125 × 0.75	8.38	–	0	−0.03
0.0625 × 1.25	4.86	−9.79	0	−0.03
0.0625 × 0.75	8.79	–	0	−0.05

Table 2. Identification of location of vertical void located at ($x_1/L = -1.8$, $x_2/L = -1.2$)

Void size	Relative percentage error in void location [%]			
	Direction of translation for functional (8)		Direction of translation for functional (9)	
	x_1	x_2	x_1	x_2
Measured temperature maximal error 0.1°C				
0.125 × 1.25	0.46	1.28	0	0.07
0.125 × 0.75	1.56	4.21	0	0.01
0.0625 × 1.25	0.65	1.69	0	0.06
0.0625 × 0.75	2.43	4.24	0	0
Measured temperature maximal error 0.2°C				
0.125 × 1.25	0.93	2.72	0	0.06
0.125 × 0.75	3.63	4.37	0	0.01
0.0625 × 1.25	1.33	3.70	0	0.06
0.0625 × 0.75	5.52	4.35	0	0

Table 3. Identification of location of horizontal void located at ($x_1/L = -1.8$, $x_2/L = -0.2$)

Void size	Relative percentage error in void location [%]			
	Direction of translation for functional (8)		Direction of translation for functional (9)	
	x_1	x_2	x_1	x_2
Measured temperature maximal error 0.1°C				
0.125 × 1.25	−0.29	–	0	−0.73
0.125 × 0.75	1.35	–	0	–
0.0625 × 1.25	−4.76	–	0	0.79
0.0625 × 0.75	−4.94	–	0	−0.81
Measured temperature maximal error 0.2°C				
0.125 × 1.25	−0.37	–	0	−0.73
0.125 × 0.75	5.59	–	0	–
0.0625 × 1.25	4.96	–	0	−0.81
0.0625 × 0.75	−4.99	–	0	−0.83

Table 4. Identification of location of horizontal void located at ($x_1/L = -1.8$, $x_2/L = -1.2$)

Void size	Relative percentage error in void location [%]			
	Direction of translation for functional (8)		Direction of translation for functional (9)	
	x_1	x_2	x_1	x_2
Measured temperature maximal error 0.1°C				
0.125 × 1.25	−0.84	0.07	0	0.01
0.125 × 0.75	−1.65	1.05	0	0
0.0625 × 1.25	−1.06	0.08	0	0
0.0625 × 0.75	2.25	1.26	0	0
Measured temperature maximal error 0.2°C				
0.125 × 1.25	−1.72	0.11	0	0
0.125 × 0.75	−4.38	2.02	0	0
0.0625 × 1.25	−2.18	0.14	0	0
0.0625 × 0.75	−4.98	2.39	0	−0.01

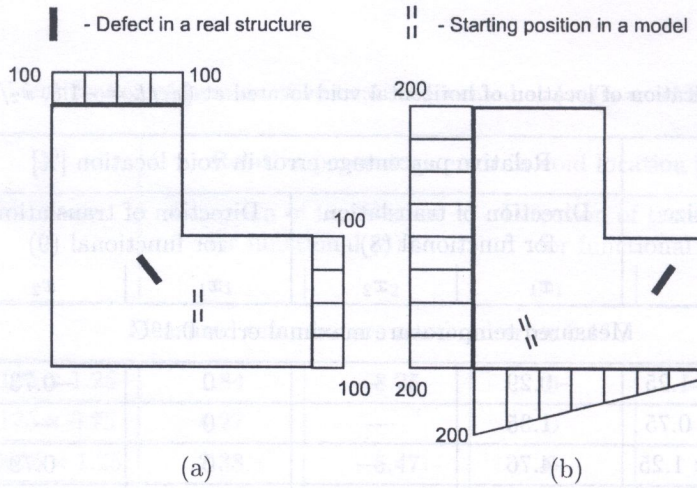

Fig. 9. Angle disk with void subjected to uniformly distributed temperature (a) and uniformly-varying distributed temperature (b)

Table 5. Identification of void located in angle disk subjected to uniform temperature along two external boundaries

Relative error of identification [%]		
Direction of translation		Angle of rotation
x_1	x_2	
Error free measurement		
1.25	0.07	0.22
Measured temperature maximal error 0.05°C		
10.6	15.87	−17.46
Measured temperature maximal error 0.1°C		
2.7	−31.56	6.12

Table 6. Identification of void located in angle disk subjected to uniform temperature along left external boundary and varying temperature along lower boundary

Relative error of identification [%]		
Direction of translation		Angle of rotation
x_1	x_2	
Error free measurement		
−0.81	2.75	3.86
Measured temperature maximal error 0.05°C		
2.75	15.87	3.86
Measured temperature maximal error 0.1°C		
2.23	2.75	3.86

In second example, an angle disk with rectangular void within its domain, cf. Fig. 9, was considered. The disk was subjected to two different sets of thermal boundary conditions, shown in Figs. 9a,b, respectively. The localization and orientation of the void should be identified, allowing for its translation and rotation in model disk. Similarly as in the previous example, the identification functional was selected in the form of 'distance norm' (8) and the measured temperature along external boundaries for 'real' disk was numerically simulated, introducing some random absolute error of measured temperature distribution into simulation. The results of identification procedure are presented in Tables 5 and 6. The obtained results indicate the similar nature of thermal identification as in the previous example.

8. Concluding remarks

The present paper is concerned with the defect or damage identification method using thermal response of a structure. Particularly, the temperature distribution caused by internally applied heat sources or prescribed temperatures on external boundaries can constitute the basis for identification of location, orientation and size of internal voids and defects within the structure domain. Since the proposed identification procedure is gradient-oriented, then the sensitivity analysis has to constitute its essential part. The class of path-independent sensitivity integrals associated with arbitrary behavioral functional in the case of steady-state heat transfer problem proposed earlier by Dems and Mróz [1], was extended for the case of transient heat transfer problem and utilized for thermal identification purposes. The detailed analysis of such approach will be presented in consecutive paper.

The success of thermal identification depends on how the change of boundary temperature distribution is sensitive to the changes in void or inhomogeneity location. This sensitivity can be influenced by the proper selection of applied boundary conditions during measurement of real structure and calculation of its model. These phenomena will be also analyzed in details in consecutive papers.

Acknowledgment

This research work was supported through Scientific Research Committee (KBN) Grant No. 3 T08C 021 29.

References

[1] K. Dems and Z. Mróz. Shape sensitivity in mixed Dirichlet-Neumann boundary-value problems and associated class of path-independent integrals,. *Eur. J. Mech. A/Solids*, **14**(2): 169–203, 1995.

[2] K. Dems, R. Korycki and B. Rousselet. Application of first- and second-order sensitivities in domain optimization for steady conduction problem. *J. Thermal Stresses*, **20**: 697–728, 1997.

[3] K. Dems and Z. Mróz. Sensitivity analysis and optimal design of external boundaries and interfaces for heat conduction systems. *J. Thermal Stresses*, **21**: 461–488, 1998.

[4] K. Dems and B. Rousselet. Sensitivity analysis for transient heat conduction in a solid body. *Struct. Opt.*, **17**: 36–45 (part I), 46–54 (part II), 1999.

[5] K. Dems, Z. Mróz. Sensitivity analysis and path-independent integrals in heat transfer problems. In: *Rozprawy z mechaniki konstrukcji i materiałów*, pp. 51–64, Wyd. Politechniki Krakowskiej, Seria: Inżynieria Lądowa, Monografia 302, Cracow 2004.

[6] S.W. Doebling, C.R. Farrar, M.B. Prime and D.W. Sheritz. Damage identification and health monitoring of structural and mechanical systems from changes in their vibration characteristics: a literature review. Los Alamos Natl. Lab. Rep. LA–13070–MS, 1996